Ultrasound in Med. & Biol., Vol. 27, No. 2, pp. 267–277, 2001

0301-5629/01/$–see front matter

PII: S0301-5629(00)00342-2

● *Original Contribution*

SUPERTHRESHOLD BEHAVIOR OF ULTRASOUND-INDUCED LUNG HEMORRHAGE IN ADULT MICE AND RATS: ROLE OF PULSE REPETITION FREQUENCY AND EXPOSURE DURATION

WILLIAM D. O'BRIEN JR.,* LEON A. FRIZZELL,* DAVID J. SCHAEFFER† and JAMES F. ZACHARY‡

*Bioacoustics Research Laboratory, Department of Electrical and Computer Engineering, University of Illinois, Urbana, IL, USA; Departments of †Veterinary Biosciences and ‡Veterinary Pathobiology, University of Illinois, Urbana, IL, USA

(*Received* 24 *May* 2000; *in final form* 18 *October* 2000)

Abstract—Superthreshold behavior for ultrasound-induced lung hemorrhage was investigated in adult mice and rats at an ultrasound center frequency of 2.8 MHz to assess the role of pulse repetition frequency and exposure duration. One hundred fifty, 6–7-week-old female ICR mice and 150 10–11-week-old female Sprague-Dawley rats were each divided into 15 exposure groups (10 animals per group) for a 3 × 5 factorial design (3 exposure durations of 5, 10, and 20 s and 5 pulse repetition frequencies of 25, 50, 100, 250, and 500 Hz). The *in situ* (at the pleural surface) peak rarefactional pressure of 12.3 MPa and the pulse duration of 1.42 μs were the same for all ultrasonically-exposed animals. In addition, 15 sham exposed mice and 15 sham exposed rats were included into both studies. In each study of 165 animals, the exposure conditions were randomized. The lesion depth and surface area were measured for each animal, as well as the percentage of animals with lesions per group. The characteristics of the lesions produced in mice and rats were similar to those described in studies by our research group and others, suggesting a common pathogenesis for the initiation and propagation of the lesions at the gross and microscopic levels. The proportion of lesions in both species was related statistically to pulse repetition frequency (PRF) and exposure duration (ED), with the exception that PRF in rats was not quite significant; the PRF × ED interaction (number of pulses) for lesion production was not significant for either species. The PRF, but not ED, significantly affected lesion depth in both species; the PRF × ED interaction for depth was not significant for either species. Both PRF and ED significantly affected lesion surface area in mice, while neither affected area in rats; the PRF × ED interaction for surface area was not significant for either species. (E-mail: wdo@uiuc.edu)

Key Words: **Ultrasound bioeffects, Mouse lung, Rat lung, Pulsed ultrasound, Lung hemorrhage.**

INTRODUCTION

The effect of exposure timing quantities such as pulse duration, exposure duration, total on-time, and pulse repetition frequency on the threshold for ultrasound-induced lung hemorrhage and on the size of the lesions at superthreshold levels has been examined to a very limited extent. Most of the studies that have considered the role of timing quantities have focused on estimating threshold levels (Child et al. 1990; Raeman et al. 1993; 1996; Frizzell et al. 1994).

There are a number of exposure timing quantities and, therefore, to avoid confusion, a clear understanding of the concept of each of these terms is necessary. Pulse duration (PD), sometimes called pulse length, represents the on-time (time duration) of an individual ultrasonic pulse, typically in the range of 1 μs for diagnostic ultrasound equipment. Pulse repetition frequency (PRF) represents the rate of the pulses, typically 1 kHz for gray-scale imaging. The reciprocal of the pulse repetition frequency is the pulse repetition period (PRP), which represents the time between the initiation of consecutive pulses. Exposure duration (ED) represents the total time that the ultrasound field is insonating (exposing) a specific tissue region, and includes both the time that the pulse is energized and the time between pulses. Total on-time represents the time that only the pulses are energized, that is, the product of pulse duration and total

Address correspondence to: William D. O'Brien Jr., Bioacoustics Research Laboratory, Department of Electrical and Computer Engineering, University of Illinois, 405 North Mathews, Urbana, IL 61801 USA. Email: wdo@uiuc.edu

number of pulses. Duty cycle represents the fractional amount of time (or percentage) that the pulse is excited (pulse duration) relative to the pulse repetition period, that is, the product of pulse duration and pulse repetition frequency.

Child et al. (1990) reported that the pressure threshold for lung hemorrhage at 3.7 MHz for a pulse duration of 1 μs was approximately twice that of a pulse duration of 10 μs (1.5-MPa vs. 3.0-MPa compressional pressure). The exposure duration (180 s) and duty cycle (0.1%) were the same; therefore, the PRF and the number of pulses were different by a factor of 10. However, in the same article (Child et al. 1990), the authors reported that, using a frequency of 1.2 MHz, pulse duration of 10 μs, and exposure duration of 180 s, where they varied only the pulse repetition frequency, and hence the duty cycle or number of pulses, they obtained the same pressure threshold (0.7 MPa). Frizzell et al. (1994) reported a decrease in threshold level with total on-time (and exposure duration) in neonatal mice at 10°C for 1-MHz pulsed ultrasound with a 10-μs pulse duration. The pressure thresholds they reported were approximately 0.37 MPa for 180-s exposure duration (100-Hz PRF) and 1.5 MPa for 2.4-s exposure duration (1-kHz PRF). Raeman et al. (1993) reported that exposure duration (3 min at 17-Hz PRF vs. 3 s at 1-kHz PRF) had a small effect on pressure threshold and extent of damage when the total on-time was held constant at 0.03 s for a pulse duration of 10 μs. Later, the same group (Raeman et. al. 1996) reported no statistically significant difference in the compressional pressure threshold (1.6 and 1.4 MPa) for ED of 20 and 180 s (10-μs pulse duration and 100-Hz PRF at 2.3 MHz), respectively.

The effect of timing quantities on superthreshold lesion development is more limited. Raeman et al. (1996) reported differences in lesion size between 20- and 180-s exposure durations, but data were not provided in the report. Earlier, Raeman et al. (1993) reported that the lesion volume in mouse lung was greater for 3-min exposure duration (100-Hz PRF) than for 0.3-min exposure duration (1000-Hz PRF), suggesting a dependence of lesion growth on exposure duration. However, the PRF was also different for the two exposures. There seems to be no published data evaluating independently the effects of PRF and ED.

Thus, the literature appears to show only a minor dependence of pressure threshold levels for ultrasound-induced lung hemorrhage on timing quantities. There is a suggestion of an effect on the superthreshold lesion size; however, little information is available. In this study, a more complete examination of the role of PRF and ED has been undertaken for superthreshold conditions to determine the effect of each variable and any interaction (number of pulses) between the two variables. The study is conducted using both mice and rats, because results of one of our earlier studies have shown a significantly larger lesion size in rats than in mice (Zachary et al. 2001), which was consistent with the greater lesion size in older (larger) when compared to younger (smaller) mice (Dalecki et al. 1997b).

This article reports the results of two similar experiments, one with adult mice and the other with adult rats, that evaluated two timing quantities (PRF and ED) under the same superthreshold exposure conditions, using the same factorial design. This is the first study to evaluate the role of PRF and ED on ultrasound-induced lung hemorrhage, and their interaction.

MATERIALS AND METHODS

Exposimetry

The exposimetry and calibration procedures have been described previously in detail (Zachary et al. 2001). Ultrasonic exposures were conducted using one focused, 19-mm-diameter, lithium niobate ultrasonic transducer (Valpey Fisher, Hopkinton, MA, USA). Water-based (distilled water, 22°C) pulse-echo ultrasonic field distribution measurements were performed according to established procedures (Raum and O'Brien 1997) and yielded a center frequency of 2.8 MHz, a fractional bandwidth of 11.6%, a focal length of 18.9 mm, a 6-dB focal beam width of 466 μm, and a 6-dB depth of focus of 2.73 mm.

An automated procedure was developed toroutinely calibrate the ultrasound fields (Sempsrott and O'Brien 1999; Sempsrott 2000; Zachary et al. 2001). The procedure was based on the Acoustic Output Measurement Standard for Diagnostic Ultrasound Equipment (AIUM/NEMA 1998) and the Standard for the Real-Time Display of Thermal and Mechanical Acoustic Output Indices on Diagnostic Ultrasound Equipment, commonly referred to as the Output Display Standard, ODS (ODS, 1998). The source transducer was mounted in a water tank (degassed water, 22°C) and its drive voltage was supplied by a RAM5000 (Ritec, Inc., Warwick, RI, USA) that had the capability to deliver up to a 5-kW single-cycle pulse into a 50-ohm load (Fig. 1). One of two calibrated PVDF membrane hydrophones (Perceptron Model 804-010, Plymouth Meeting, PA, USA and Marconi Model Y-34-6543, Chelmsford, UK) was mounted to the computer-controlled micropositioning system (Daedal, Inc., Harrisburg, PA, USA). Each of the three orthogonal axes of the micropositioning system has a linear accuracy of 2 μm. The hydrophone's signal was digitized with an oscilloscope (500 Ms/s, LeCroy Model 9354TM, Chestnut Ridge, NY, USA), and transferred to the same computer (Dell Pentium II) that controlled the positioning system.

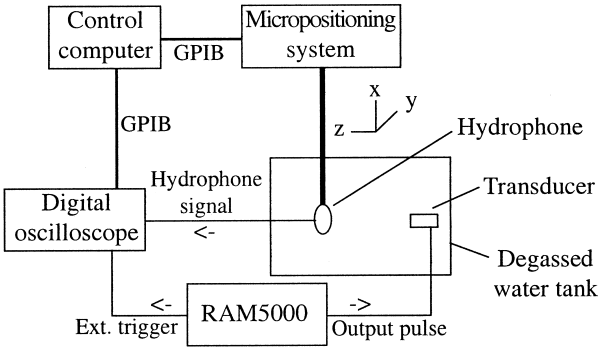

Fig. 1. Block diagram of ultrasound calibration procedure.

Table 1. The *in situ* (at the pleural surface) peak rarefactional pressure $p_{r(in\ situ)}$ and peak compressional pressure $p_{c(in\ situ)}$

	Mouse exposures		Rat exposures	
	Sham	Exposed	Sham	Exposed
$P_{r(in\ vitro)}$ (MPa)	0.26	13.2	0.26	14.6
$P_{c(in\ vitro)}$ (MPa)	0.30	20.9	0.30	24.4
$p_{r(in\ situ)}$ (MPa)	0.24	12.3	0.22	12.3
$p_{c(in\ situ)}$ (MPa)	0.28	18.9	0.25	20.6
MI	0.12	6.3	0.12	7.1

All animals were exposed to pulsed ultrasound (1-kHz pulse repetition frequency and 10-s exposure duration). The sham exposure conditions used a pulse repetition frequency of 10 Hz. The mechanical index is provided because this is a regulated quantity of diagnostic ultrasound equipment (FDA 1997).

The pulse intensity integral (PII) is the basic field quantity used to estimate the beam axis for which the instantaneous acoustic pressure was determined from the calibrated hydrophone. The PII was calculated for each pulse. The 2.8-MHz source transducer's beam axis was estimated using an automated procedure that yielded (via a linear regression analysis) an equation for the beam axis. The control computer used the beam axis equation (Zachary et al. 2001) to acquire RF hydrophone waveforms at 50-μm intervals along the 8 mm of the beam axis that included the focal region. The acquisition rate was 500 Ms/s. The only exception to the calibration procedure as discussed above was the insertion of a 13-ohm in-line attenuator between the RAM5000 and transducer; this configuration was used for sham exposures to yield a very low exposure level during transducer alignment procedures. The RF data were transferred to a Sun UltraSparc workstation and analyzed using Matlab® (The Mathworks, Natick, MA, USA).

The RF hydrophone waveforms were processed to yield axial profiles for the following quantities: rarefactional pressure, compressional pressure, pulse intensity integral, and their derated (0.3 dB/cm-MHz) values. From these profiles, the following water-based exposure quantities were determined: the peak rarefactional pressure $p_{r(in\ vitro)}$, the peak compressional pressure $p_{c(in\ vitro)}$, the derated (0.3 dB/cm-MHz) peak rarefactional pressure $p_{r.3}$, and the derated (0.3 dB/cm-MHz) peak compressional pressure $p_{c.3}$. Both $p_{r.3}$ and $p_{c.3}$ were determined at the location of the maximum value of the derated pulse intensity integral. The mechanical index was calculated using the ODS procedure (ODS, 1998) from

$$p_{r.3}/\sqrt{f_c} \tag{1}$$

where f_c is the center frequency of 2.8 MHz (see Table 1). A total of 25 independent calibrations of the 2.8-MHz transducer were conducted before, during, and after the 5-month period of the experiments. At the exposure levels used in this study, the relative standard deviation (SD $\times$ 100/mean) of was 16.5% for $p_{r(in\ vitro)}$ and 19.5% for $p_{c(in\ vitro)}$.

The purpose for providing the mechanical index (MI) in Table 1 is because it is a regulated quantity (FDA 1997) of diagnostic ultrasound systems, and its magnitude is available to system operators. Thus, there is value to provide the MI in order to give general guidance to manufacturers and operators as to the levels we are using in this study.

The *in situ* (at the pleural surface) peak rarefactional and compressional pressures were estimated from

$$p_{r(in\ situ)} = p_{r(in\ vitro)}e^{-(A\cdot x)} \tag{2}$$

and

$$p_{c(in\ situ)} = p_{c(in\ vitro)}e^{-(A\cdot x)}, \tag{3}$$

respectively, where $p_{r(in\ vitro)}$ and $p_{c(in\ vitro)}$ are the maximum water-based values, A is the mean insertion loss of the chest wall (2.8 dB/cm at 2.8 MHz) measured from 41 separate mouse chest walls and 27 separate rat chest walls using a broadband insertion loss technique (Teotico et al. 2001), and x is the mean chest wall thickness.

The experimental protocol required the same *in situ* (at the pleural surface) peak rarefactional pressure $p_{r(in\ situ)}$ for all exposed animals. Mouse and rat chest wall insertion losses and thicknesses were used from previous experiments (Teotico et al. 2001; Zachary et al. 2001) to estimate the various $p_{r(in\ vitro)}$ values that would correspond to the same $p_{r(in\ situ)}$ value. The actual $p_{r(in\ situ)}$ values obtained in this study were determined from the measured chest wall thicknesses of the animals used

herein, and the chest wall insertion losses were those previously determined (Teotico et al. 2001). Thus, for both the mouse and rat studies, $p_{r(in\ situ)}$ was 12.3 MPa, the quantity used for the study protocol.

Animals

The experimental protocol was approved by the campus' Laboratory Animal Care Advisory Committee and satisfied all campus and NIH rules for the humane use of laboratory animals. Animals were housed in an AAALAC-approved animal facility, placed in groups of three or four in polycarbonate cages with beta-chip bedding and wire bar lids, and provided food and water *ad libitum*.

In the mouse experiment, a total of 165 6–7-week-old 22.2 ± 0.2-gram female ICR mice (Harlen Sprague Dawley Laboratories, Indianapolis, IN, USA) were divided into 15 ultrasonically-exposed groups (10 mice per group) and one sham group (15 mice). The experiment was a 3×5 factorial design with three exposure duration groups and 5 pulse repetition frequency groups. Mice were randomly divided among the 16 different groups. In the rat experiment, a total of 165 10–11-week-old 293 ± 28-gram female Sprague-Dawley rats (Harlan) were grouped identically to those animals used in the mouse experiment. The *in situ* peak rarefactional pressure was the same for all ultrasonically-exposed groups. The individuals involved in animal handling, exposure, and lesion scoring were blinded to the exposure condition. The exposure conditions for each animal were revealed only after the final results were tabulated.

Mice and rats were weighed and then anesthetized with ketamine hydrochloride (87.0 mg/kg) and xylazine (13.0 mg/kg) administered IP. For each animal, the skin of the left thorax was exposed by removing the hair with an electric clipper, followed by a depilatory agent (Nair® Carter-Wallace, Inc., New York, NY, USA) to maximize sound transmission. A black dot was placed on the skin over the ribs at approximately the sixth to ninth rib to guide the positioning of the ultrasonic beam. Anesthetized animals were placed in specially designed holders that were sized for each species. The ultrasonic transducer was attached to the holder. A removable pointer, attached to the transducer, was used to position the ultrasonic beam perpendicular to the skin at the position of the black dot with the beam's focal region approximately at the lung surface (Fig. 2).

The holder with the animal and mounted transducer was placed in degassed, temperature-controlled (30°C) water. The low-power pulse-echo capability of the exposure system (RAM5000, Ritec, Inc., Warwick, RI, USA) displayed on an oscilloscope was used to adjust the axial center of the focal region to within 1 mm of the lung surface. It was during this part of the experimental procedure that the 13-ohm in-line attenuator was placed between the RAM5000 and transducer to obtain very low exposure values (see Table 1). Also, the pulse repetition frequency was 10 Hz during this alignment procedure. All ultrasonically-exposed animals received the same *in situ* peak rarefactional pressure $p_{r(in\ situ)}$ of 12.3 MPa. Exposure duration (5, 10, and 20 s) and pulse repetition frequency (25, 50, 100, 250, and 500 Hz) were randomly assigned to each animal. During the exposure, each animal was observed for changes in its breathing pattern and respiratory rate. Following exposure, animals were removed from the water and holder, and then euthanized under anesthesia by cervical dislocation.

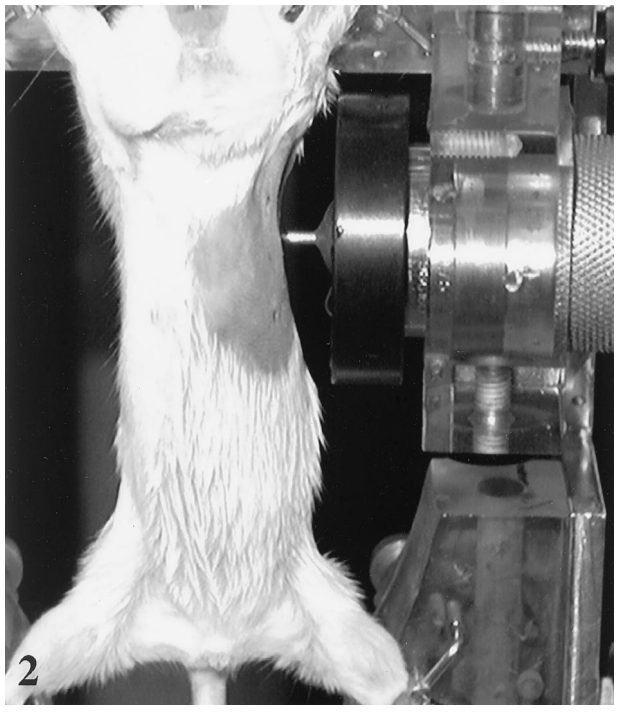

Fig. 2. Apparatus used to hold, position, and align the transducer's field on the left lung of the experimental animal, shown here for a mouse. A removable pointer, placed over the transducer, is used to position the ultrasonic beam perpendicular to the skin in the beam's focal region. The tip of the pointer is aligned with a black dot placed on the skin in the intercostal space between the ribs.

The thorax was opened and the thickness of each left thoracic wall (skin, rib cage, and parietal pleura) at the point of exposure was measured using a digital micrometer (accuracy: 10 μm). These chest wall measurements were used for later calculation of the *in situ* ultrasonic pressures at the visceral pleural surface. The lungs were removed from each animal and the left lung lobe was scored for the presence or absence of hemorrhage. The left lung was fixed by immersion in 10% neutral-buffered formalin for a minimum of 24 h. After

fixation, the elliptical dimensions of each lung lesion at the visceral pleural surface were measured using a digital micrometer where "a" is the semi-major axis and "b" is the semi-minor axis. The lesion was then bisected and the depth "d" of the lesion within the pulmonary parenchyma was also measured. The surface area (πab) and volume (πabd/3) of the lesion were calculated for each animal. Each half of the bisected lesion was embedded in paraffin, sectioned at 5 μm, stained with hematoxylin and eosin, and evaluated microscopically.

Statistics

Exploratory data analyses of the proportion of lesions, and lesion depth, surface area, and volume included: examination of summary statistics for various treatment groups, bivariate plots of each lesion characteristic against pulse repetition frequency (PRF) and exposure duration (ED) individually, contour plots of each lesion characteristic against PRF and ED jointly, and probability plots. To obtain a better approximation to a normal distribution, lesion volumes were transformed as volume$^{0.25}$. The primary questions concerned the effects of PRF and ED on the proportion of lesions, and lesion depth, surface area, and volume, for each species separately. These were analyzed by factorial analysis of variance for each species separately (Snedecor and Cochran 1989). Differences between species were determined using factorial analysis of variance that included species as the third factor. Additional analyses were carried out using analysis of covariance (ANCOVA) (Snedecor and Cochran 1989). ANCOVA was used to determine if the shapes of the regression relationships between lesion parameters against the PRF differed between the treatments given by ED. Pearson's correlation was used to determine the strength of the relationship between lesion area and lesion depth (Snedecor and Cochran 1989). *p*-values were considered significant at the 5% level.

RESULTS

Clinical observations

There were no clinical observations to report.

Chest wall thickness

The mean ($\pm$SD) thickness of the left thoracic wall (skin, rib cage, and parietal pleura) at the point of exposure were 2.22 $\pm$ 0.19 mm (165 mice) and 4.54 $\pm$ 0.38 mm (165 rats). These thickness values, along with previously determined chest wall insertion losses (Teotico et al. 2001), yielded $p_{r(in\ situ)}$ = 12.3 MPa for both the mouse and rat exposures.

Gross and histological observations

Grossly, the lesion visible on the visceral pleural surface was a red to dark red elliptical area of hemorrhage that formed along the pathway of the ultrasound beam (Fig. 3). Examination of the bisected lesion demonstrated hemorrhage that assumed a conical shape whose base opposed the visceral pleural surface and whose apex extended into subjacent lung parenchyma to varied depths within the lung. The surface area of the lesion at the pleural surface was correlated with the depth of the lesion into the subjacent lung parenchyma for both species.

Microscopically, the lesion was alveolar hemorrhage; alveolar septa did not appear injured. The principal tissue affected was the microvasculature. There were no differences in the gross or microscopic characteristics of the lesion based on species exposed, except for those characteristics (depth, surface area) determined by exposure conditions (PRF and ED). In all animals, especially those receiving the fewest pulses (PRF $\times$ ED interaction), the initial site of hemorrhage was the alveoli immediately subjacent to the exposed visceral pleura. The visceral pleura had no lesions. Alveoli were packed with erythocytes and occasional accretions of plasma proteins. Under these exposure conditions, alveoli deeper within lung parenchyma, but in the exposure area contained less or no hemorrhage.

Analysis of lesion shape

As in our previous studies (O'Brien et al. 2000; Zachary et al. 2001), none of the shams (mice: $n = 15$; rats: $n = 15$) had lesions. Comparison of lesion depth and surface area was done for two conditions, one using all of the exposed animals and the other using only the exposed animals that had lesions. Lesion depth and surface area were correlated in each species (mice: $n = 150$; rats: $n = 150$; shams excluded; Pearson's correlation coefficient R = 0.7; $p < 0.0001$). In animals that had lesions (shams excluded), Pearson's correlation coefficients between lesion depth and surface area were significant (mice: R = 0.51, $p < 0.0001$, $n = 103$; rats: R = 0.60, $p < 0.0001$, $n = 121$). Lesion volume is not an independent measure of lesion size because lesion depth and surface area are highly correlated.

Proportion (percent) of animals with lesions

As pulse repetition frequency and/or exposure duration increased, the percentage of animals with lesions approached 100% for both species (Fig. 4). Factorial analysis of variance (Table 2) showed that lesion production in mice and rats was related to PRF and ED, with the exception that PRF in rats was not significant. The PRF $\times$ ED interaction was not significant for either species (although it was borderline significant in rats). Arithmetically, the PRF $\times$ ED interaction is the total number of pulses, and a not significant interaction suggests that the effects due to the number of pulses are

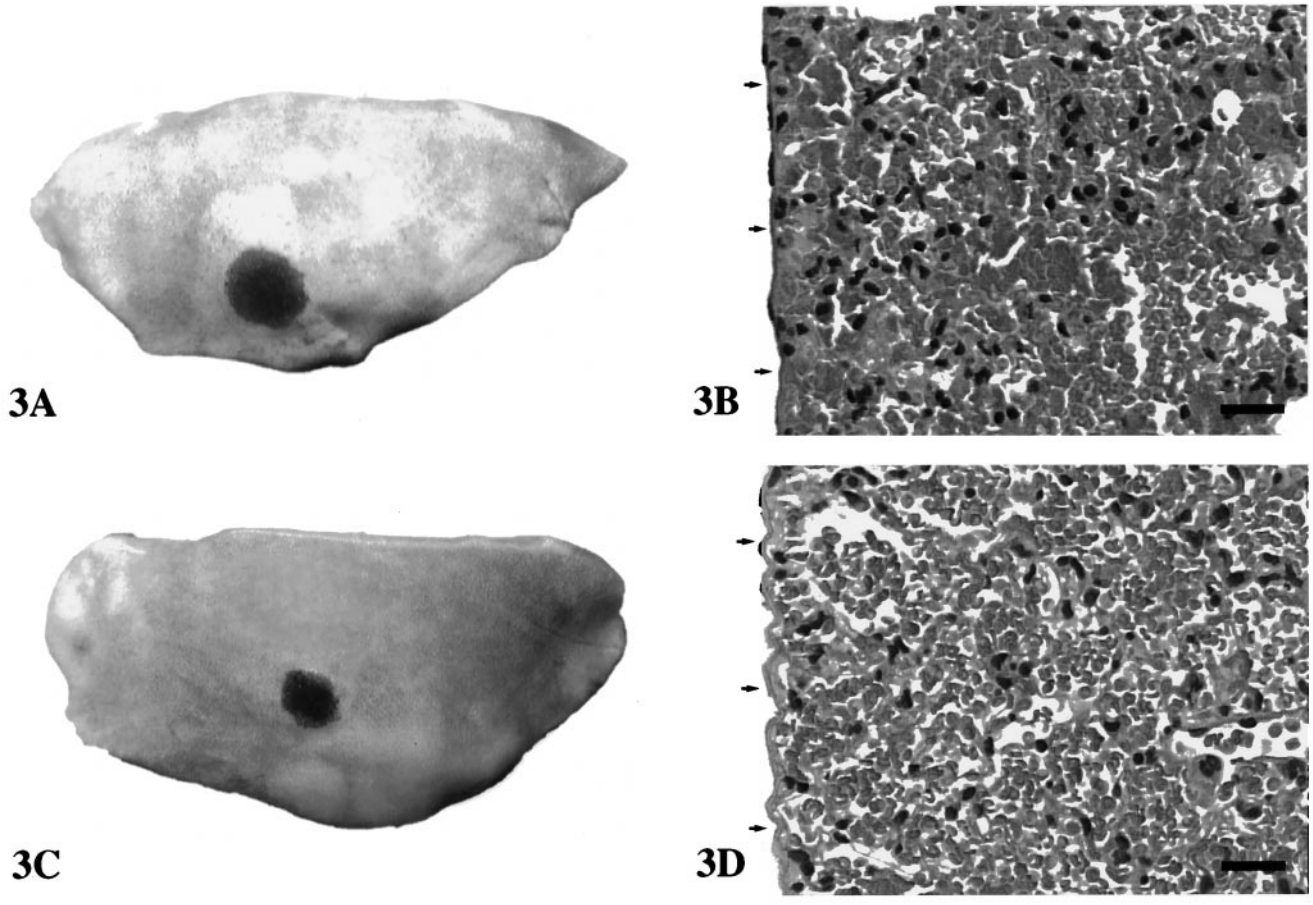

Fig. 3. Mouse (A, B) and rat (C, D) lungs exposed to pulsed ultrasound. Grossly (left panel), the lesion on the surface of the mouse (A) and rat (C) lung is a red to dark red expansile elliptical area of hemorrhage. The visceral pleura is intact. Histologically (right panel), the lesion in mouse (B) and rat (D) lung is alveolar hemorrhage; alveolar septa and visceral pleura are not injured (arrows). Lesions are similar in character in both mice and rats, but vary in severity based on exposure conditions. Bar = 300 μm.

additive from the individual observations (PRF and/or ED).

Lesion depth, surface area, and volume

The PRF, but not ED, significantly affected lesion depth in both species (Table 2; Fig. 5). Also, the PRF × ED interaction for depth was not significant for either species.

Both PRF and ED significantly affected lesion surface area in mice, while neither affected area in rats (Fig. 6). Also, the PRF × ED interaction for surface area was not significant for either species.

As noted earlier, lesion volume was not an independent variable. Nevertheless, PRF and ED significantly affected lesion volume in mice, PRF but not ED significantly affected lesion volume in rats, and the PRF × ED interaction for volume was not significant for either species (Fig. 7).

As an aid to interpreting these results, analysis of covariance (ANCOVA) was carried out for each measure of lesion size for both species separately, using PRF as a linear regression variable and ED as a treatment variable. For mice, the slopes of the regression curves (lesion size measure versus PRF) were parallel and significant. For mice, treatments (*i.e.*, ED) were not significantly different for depth, but were significant for volume$^{0.25}$ ($p < 0.01$) and were marginally significant for area. For each measure of lesion size in rats, the slopes were parallel and significant ($p < 0.01$), and the treatments (*i.e.*, ED) did not differ significantly.

Species was not included in the randomized factorial design; each species was exposed separately for experimental convenience. As clearly seen in the figures and in Table 2, species significantly affected lesion proportions (Fig. 4) and size (Figs. 5, 6, and 7).

The PRF × ED interaction term, that is, the number

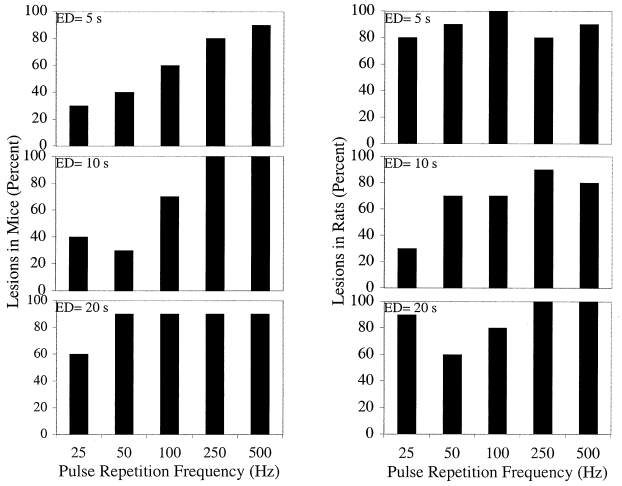

Fig. 4. Percentage of lesions in mice (left panels) and rats (right panels) as a function of pulse repetition frequency for the three exposure durations.

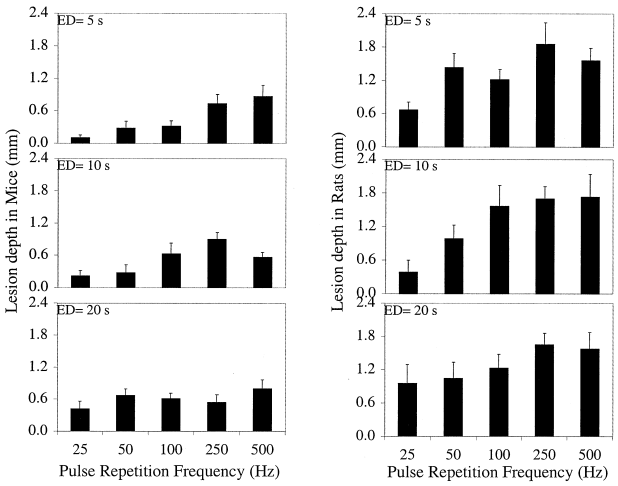

Fig. 5. Mean lesion depth in mice (left panels) and rats (right panels) as a function of pulse repetition frequency for the three exposure durations. Error bars represent SEM.

of pulses, is graphically shown for completeness (Fig. 8). This figure shows very little difference for proportion of lesions, but clearly demonstrates a difference between mice and rats for lesion size.

DISCUSSION

The value of $p_{r(in\ situ)}$ selected for this study had to be large enough to ensure a sufficient number of lesions in order to test the dependency of lesion formation and size on PRF and ED. The $p_{r(in\ situ)}$ value of 12.3 MPa was based on our previous findings (Zachary et al. 2001) in which the percentage of mice and rats with lesions was 80% at an ultrasonic frequency of 2.8 MHz, and a $p_{r(in\ situ)}$ of about 11 MPa. In this previous study, the PRF was 1 kHz and the ED was 10 s, which yielded 10000 pulses per exposure. The study design herein used a total number of pulses between 125 and 10000. Thus, the previous study's findings determined the maximum number of pulses used in this study. Therefore, it was our view that we needed to use a relatively high $p_{r(in\ situ)}$ value because the exposure conditions used herein (based on total number of pulses) were equal to or less than those in our previous study. We recognized that a

Table 2. Factorial analysis of variance results

	Probability of significant effect			
Statistical effect	Lesion proportion	Depth	Surface area	Volume*
Mouse				
PRF (25, 50, 100, 250, 500 Hz)	< 0.0001	< 0.0001	< 0.0001	< 0.0001
ED (5, 10, 20 s)	< 0.05	NS	< 0.001	< 0.01
PRF × ED	NS	NS	NS	NS
Rat				
PRF (25, 50, 100, 250, 500 Hz)	0.059	< 0.0001	NS	< 0.001
ED (5, 10, 20 s)	< 0.05	NS	NS	NS
PRF × ED	0.054	NS	NS	NS
Mouse and Rat				
Species (mouse vs. rat)	< 0.05	< 0.0001	< 0.0001	< 0.0001
PRF (25, 50, 100, 250, 500 Hz)	< 0.0001	< 0.0001	< 0.0001	< 0.05
ED (5, 10, 20 s)	< 0.01	NS	NS	NS
Species × PRF	NS	NS	NS	NS
Species × ED	< 0.05	NS	NS	NS
PRF × ED	NS	NS	NS	NS
Species × PRF × ED	< 0.05	NS	NS	NS

*Lesion volume data were transformed as volume$^{0.25}$ for ANOVA.
NS denotes not significant.

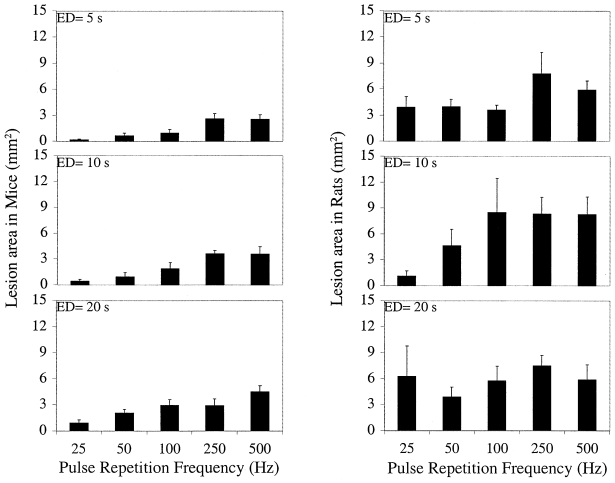

Fig. 6. Mean lesion surface area in mice (left panels) and rats (right panels) as a function of pulse repetition frequency for the three exposure durations. Error bars represent SEM.

$p_{r(in\ situ)}$ of 12.3 MPa was considerably greater than that allowed under current regulations (FDA 1997). At this $p_{r(in\ situ)}$ value, the equivalent mechanical indices for mice and rats were, respectively, 6.3 and 7.1, whereas the regulatory limit is 1.9 for diagnostic ultrasound equipment that falls under FDA control.

The characteristics of the lesions produced in mice and rats (Fig. 3) in this study were similar to those described in previous studies (Child et al. 1990; Raeman et al. 1993; Frizzell et al. 1994; Zachary and O'Brien 1995; Holland et al. 1996; Dalecki et al. 1997a; O'Brien et al. 2000; Zachary et al. 2001). Analysis of lesions and

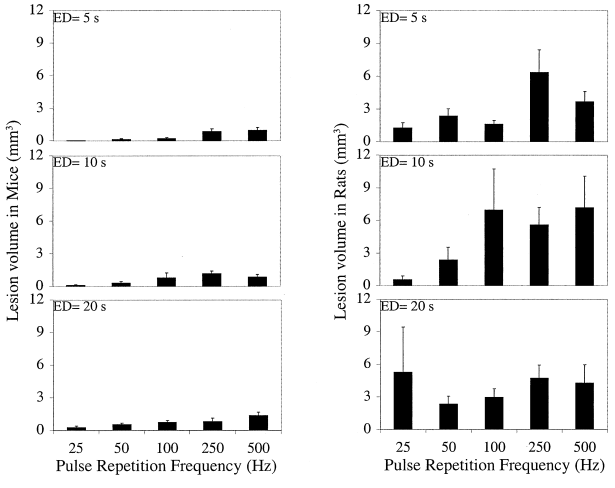

Fig. 7. Mean lesion volume in mice (left panels) and rats (right panels) as a function of pulse repetition frequency for the three exposure durations. Error bars represent SEM.

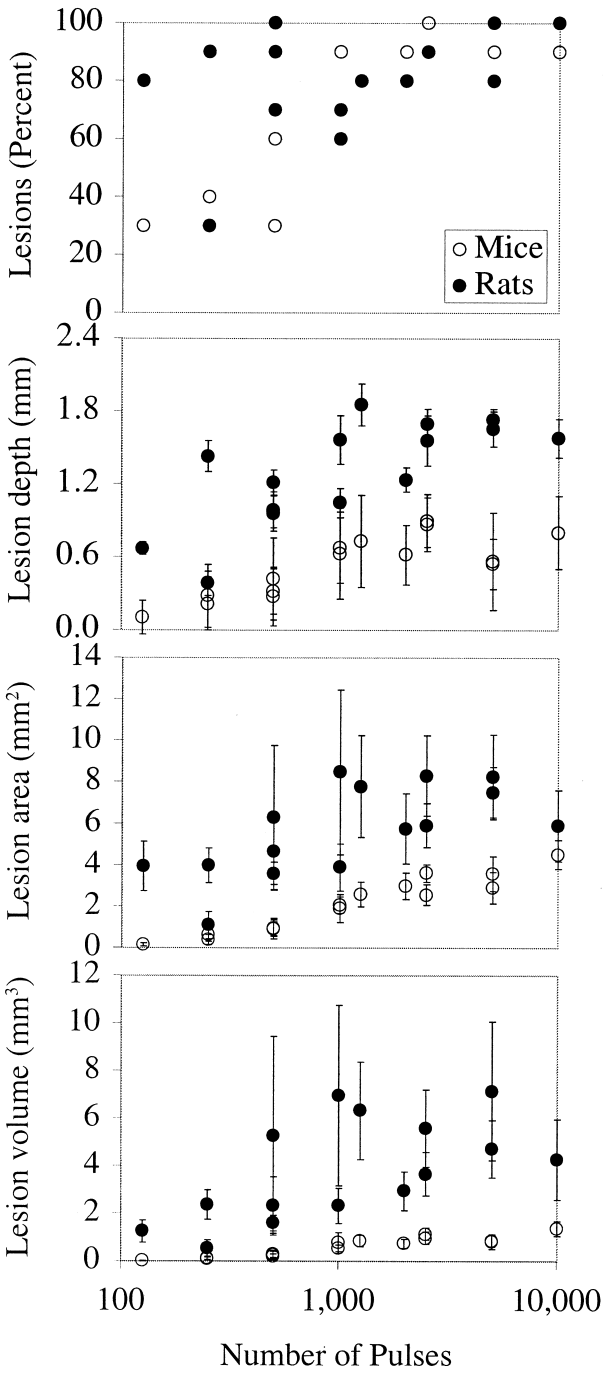

Fig. 8. Percentage of lesions, mean lesion depth, mean lesion surface area, and mean lesion volume for mice and rats as a function of the number of pulses. Error bars represent SEM.

the development of a hypothesis regarding the mechanism of injury must account for the observations made in these studies. The absence of lesions in the visceral pleura suggests that this layer behaves as a homogeneous transmitter of sound energy and thus lacks significant

impedance differences. Evaluation of ultrasound-exposed tissues by light microscopy has essentially ruled out causes such as thermal mechanisms, inertial cavitation, or other mechanical or biological phenomena that would result in massive destruction of tissues and cells.

In this study, the observation that animals that received few pulses (PRF × ED interaction term) had hemorrhage in alveoli contiguous with the visceral pleura suggests that this tissue-air layer (interface) might be the site of lesion initiation. Although a lesion resulting in alveolar hemorrhage must arise from injury to capillary endothelium and alveolar epithelial cell membranes (air-blood barrier), in all studies to date, light microscopy has not demonstrated significant pathologic alterations of cell membranes or cell nuclei to significantly account for alveolar hemorrhage. These observations suggest that the initiating lesion may not destroy entire cells or tissue layers but may act focally to damage cell membranes by forming punctate- and/or laceration-like injury. Lesions of such character would not be visible with light microscopy, and would be rapidly plugged (healed) by platelets and fibrin following the initiation of the coagulation cascade, thus limiting the severity of the hemorrhage. The production of punctate- and/or laceration-like lesions at the subcellular level following exposure to pulsed ultrasound are supported by electron microscopic studies (Penny et al. 1993).

The most plausible target for initiation of the lesions is the air-blood barrier (interface) formed (1) just under the visceral pleura, (2) at bifurcation of alveolar septa from the visceral pleura, and (3) in septa forming alveoli just under the visceral pleura. The elliptical shape of the lesion on the lung surface suggests that the lesion originates from a small point just under the visceral pleura and spreads out laterally and in depth from that point into adjacent lung parenchyma. The conical expansion of the lesion to form the apex of the cone in deeper lung tissue suggests a uniform propagation of the lesion and of ultrasound energy into these lung tissues. This conical shape implies that the sound is transferred in a uniform pattern in a homogeneous medium (alveoli filled with blood). The lesion is thus propagated into adjacent lung through repetitive waves of initiation events at the tissue-air interfaces and spreads through blood-filled alveoli to the next interface. The size of the lesion may be limited in depth by attenuation of sound energy in blood-filled alveoli and by loss of energy associated with beam spreading beyond the focal point at the visceral pleural surface, as it penetrates deeper into the lung.

In the mouse, there was a clear increase in percentage of animals with lesions with both PRF and ED (Fig. 4). However, at the largest ED of 20 s, the percentage of animals with lesions had plateaued at 90%, even at the low PRF of 50 Hz. Because there is an upper bound of 100% for percent of animals with lesions, this type of plateauing is to be expected at the higher exposures. For the rat, the proportion of animals with lesions was greater than for the mouse for similar exposure conditions (Fig. 4), despite the fact that the threshold for lesion formation has been shown to be essentially the same for the two species (Zachary et al. 2001). In addition, the plateauing of the percentage of animals with lesions with PRF seen in the mouse at an ED of 20 s is seen in the rat at essentially all EDs, but especially at EDs of 5 and 20 s. This finding is likely the reason that the results for the rat did not show a clear statistical significance with respect to PRF. Given the results in the rat it might be concluded that a lower $p_{r(in\ situ)}$ than 12.3 MPa (and lower values for percent of animals with lesions) might have given a clearer picture of the dependence on PRF and ED in rats, which might be expected to follow that of the mouse.

The dependence of lesion occurrence on PRF is supported by results of Child et al. (1990) by an examination of their Fig. 11 that shows a slightly larger proportion of mice with lesions for 100-Hz PRF as compared to 10-Hz PRF (1.2 MHz, 10-μs PD, and 180-s ED). Results of Raeman et al. (1996) showed a greater proportion of mice with lesions for a 180-s ED as compared to a 20-s ED (2.3 MHz, 10-μs PD, and 100-Hz PRF) supporting the effect of ED seen in this study. Further support for the effect of ED was given by Frizzell et al. (1994), who showed a greater percentage of lesions in neonatal mouse lungs (1 MHz, 10-μs PD) at 180-s ED (100-Hz PF) than at 2.4-s ED (1-kHz PRF); however, the PRF was different for the two EDs.

Lesion development in the mouse was clearly dependent upon PRF whereas surface area, but not lesion depth, was dependent upon ED (Table 2 and Figs. 5–7). In the rat, the picture is less clear regarding dependence on PRF because that was significant for lesion depth but not lesion area, although the rat results confirm the lack of dependence on ED for the range of EDs used in this study. The lack of dependence on ED seen in these results contrasts with results of Raeman et al. (1993) who showed a significantly larger area of hemorrhage for a 3-min ED than for one 3-s ED or three 1-s EDs (1.2 MHz, 10-μs PD); however, the PRF was different for the 3-min ED versus the other exposure durations and our results show a significant dependence on the PRF. In the same article, Raeman et al. (1993) showed that the lesion volume was greater for 3-min ED than for 0.3-min ED, although the PRF was changed from 100 Hz to 1000 Hz, respectively, to maintain the same total on-time. It may also be significant that Raeman et al. (1993) used a much larger range of ED than was used in this study; their longest ED was 180 s compared to our longest ED of 20 s.

The number of pulses is the product of the PRF and

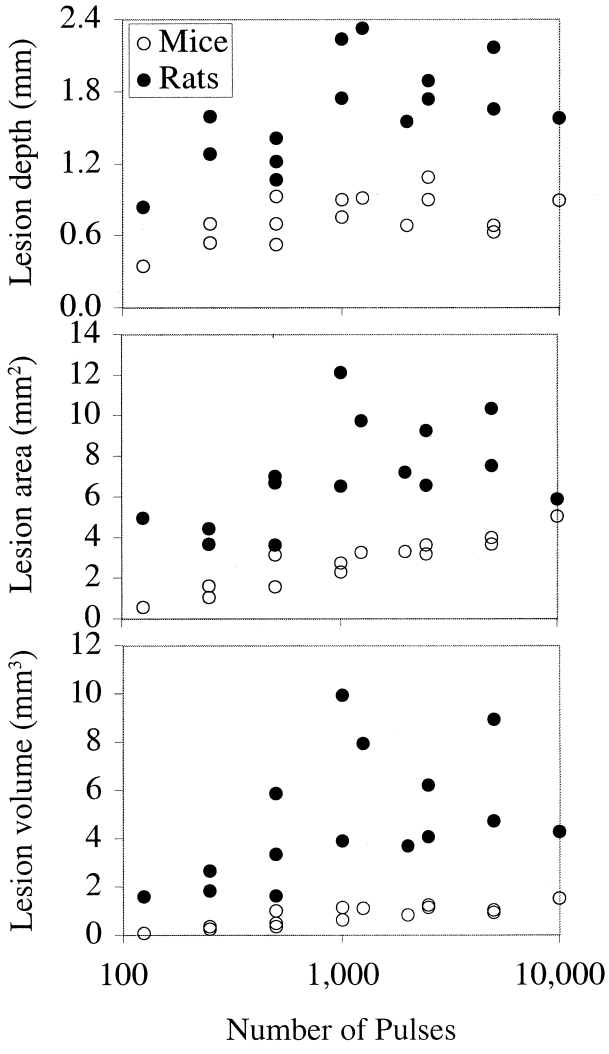

Fig. 9. Mean lesion depth, mean lesion surface area, and mean lesion volume for mice and rats as a function of the number of pulses. These data only include the animals for which there were lesions.

ED, and, given that the PD in this study was constant, is proportional to the total on-time. The number of pulses (and total on-time) is seen to have an effect on lesion percentage and lesion progression in this study (Fig. 8). Further, for lesion size there is a difference between the rat and the mouse. Interestingly, the dependence of lesion size on the number of pulses disappears above approximately 1000 pulses, for example, the lesion size increases with number of pulses below 1000 but appears to plateau and be independent of number of pulses above this number. Note that this coincides with the percentage of lesions reaching approximately 100%. Thus, this outcome might be expected when lesion size is based on all animals and not just those with lesions. However, an evaluation of only those animals that had lesions shows that this is not the case (Fig. 9).

Prior to this study, the effect of PRF and, to a lesser degree, ED on lesion progression in the lung was largely unstudied. Our results have shown a clear effect of PRF and a less significant effect of ED, over the range of EDs used in this study. The fact that the PRF and ED both affect the percentage of animals with lesions suggests that these timing quantities should be considered within the definition of the MI, which applies to nonthermal mechanisms such as that operative in lung hemorrhage. The data from this study and others are not yet sufficient to completely define the timing effects (for example, the effect of PD was not examined in this study); however, they indicate that there should be further examination of timing quantities.

Acknowledgements—We thank our valued colleagues, D. Abano, R. Bashyal, J. Blue, J. Brown, T. Bruns, J. Christoff, K. Clements, C. Frazier, H. Luo, B. McNeill, R. Miller, K. Norrell, J. Sempsrott, G. Teotico, L. Tuazon, A. Wunderlich, and B. Zierfuss, for technical contributions. This work was supported by NIH Grant HL58218 awarded to WDO and JFZ.

REFERENCES

AIUM/NEMA. Acoustic output measurement standard for fiagnostic ultrasound equipment. Laurel, MD: American Institute of Ultrasound in Medicine; and Rosslyn, VA: National Electrical Manufacturers Association, 1998.

Child SZ, Hartman CL, Schery LA, Carstensen EL, et al. Lung damage from exposure to pulsed ultrasound. Ultrasound Med Biol 1990; 16:817–825.

Dalecki D, Child SZ, Raeman CH, Cox C, Carstensen, EL, et al. Ultrasonically induced lung hemorrhage in young swine. Ultrasound Med Biol 1997a; 23:777–781.

Dalecki D, Child SZ, Raeman CH, et al. Age dependence of ultrasonically-induced lung hemorrhage in mice. Ultrasound Med Biol 1997b; 23:767–776.

FDA. Information for manufacturers seeking marketing clearance of diagnostic ultrasound systems and transducers.Rockville, MD: Center for Devices and Radiological Health, US Food and Drug Administration, September 30, 1997.

Frizzell LA, Chen E, Lee C. Effects of pulsed ultrasound on the mouse neonate: Hind limb paralysis and lung hemorrhage. Ultrasound Med Biol 1994; 20:53–63.

Holland CK, Deng CX, Apfel RE, et al. Direct evidence of cavitation *in vivo* from diagnostic ultrasound. Ultrasound Med Biol 1996; 22:917–925.

O'Brien WD Jr, Frizzell LA, Weigel RM, Zachary F, et al. Ultrasound-induced lung hemorrhage is not caused by inertial cavitation. J Acoust Soc Am 2000; 108:1290–1297.

ODS. Standard for real-time display of thermal and mechanical acoustic output indices on diagnostic ultrasound equipment. Rev. 1. Laurel, MD: American Institute of Ultrasound in Medicine; and Rosslyn, VA: National Electrical Manufacturers Association, 1998.

Penney DP, Schenk EA, Maltby K, et al. Morphologic effects of pulsed ultrasound in the lung. Ultrasound Med Biol 1993; 19:127–135.

Raeman CH, Child SZ, Dalecki D, Cox C, Carstensen EL, et al. Exposure-time dependence of the threshold for ultrasonically induced murine lung hemorrhage. Ultrasound Med Biol 1996; 22: 139–141.

Raeman CH, Child SZ, Carstensen EL. Timing of exposures in ultrasonic hemorrhage of murine lung. Ultrasound Med Biol 1993; 19:507–512.

Raum K, O'Brien WD Jr. Pulse-echo field distribution measurement technique of high-frequency ultrasound sources. IEEE Trans Ultrason Ferroelec Freq Contr 1997; 44:810–815.

Sempsrott JM, O'Brien WD Jr. Experimental verification of acoustic saturation. Proceedings of the 1999 IEEE Ultrasonics Symposium, 1999;1287–1290.

Sempsrott JM. Experimental evaluation of acoustic saturation [M.S. thesis]. Urbana, IL: University of Illinois; 2000.

Snedecor GW, Cochran WG. Statistical methods. (8th ed.) Ames, IA: Iowa State University Press, 1989.

Teotico GA, Miller RJ, Frizzell LA, Zachary JF, O'Brien WD Jr. Attenuation coefficient estimates of mouse and rat chest wall. IEEE Trans Ultrason Ferroelec Freq Contr 2001;48.

Zachary JF, O'Brien WD Jr. Lung lesion induced by continuous- and pulsed-wave (diagnostic) ultrasound in mice, rabbits, and pigs. Vet Pathol 1995; 32:43–45.

Zachary JF, Sempsrott JM, Frizzell LA, Simpson DG, O'Brien WD Jr. Superthreshold behavior and threshold estimation of ultrasound-induced lung hemorrhage in adult mice and rats. IEEE Trans Ultrason Ferroelec Freq Contr 2001;48.